

Fig. 2. Projection de quatre mailles adjacentes de la structure de $\text{NaH}_2\text{As}_3\text{O}_9$ sur le plan (100).

ment par les cations Na^+ entourés chacun de six oxygènes en un arrangement octaédrique déformé. Les octaèdres NaO_6 sont groupés par paires centro-symétriques ayant une arête commune. Chaque paire Na_2O_{10} est liée à dix polyèdres AsO_4 ou AsO_6 appartenant à quatre chaînes $(\text{H}_2\text{As}_3\text{O}_9)_n^{n-}$, par mise en commun d'un sommet oxygène avec chacun d'eux. Ces dix polyèdres comprennent quatre tétraèdres AsO_4 appartenant à des cycles As_4O_{14} , quatre tétraèdres AsO_4 bidentates et deux octaèdres AsO_6 .

Les liaisons hydrogènes contribuent également à la cohésion des chaînes. La moyenne des distances $\text{Na}-\text{O}$ dans les octaèdres NaO_6 est 2,435 Å. On constate que les liens entre chaînes sont comparativement plus faibles que ceux existant dans la chaîne, assurés par les tétraèdres AsO_4 bidentates (moyenne des distances $\text{As}-\text{O}$: 1,69 Å). Ce fait est confirmé par la texture fibreuse signalée en *Introduction*.

En récapitulant les différents arrangements que nous avons mis en évidence pour l'anion cyclique As_4O_{14} ou pour son homologue $\text{As}_2\text{V}_2\text{O}_{14}$, dans lequel les deux arsenics en coordination octaédrique ont été remplacés par des vanadiums, il apparaît que ces cycles se manifestent isolés, c'est-à-dire ne formant pas de ponts oxygènes entre eux, dans les structures de $\text{BaH}_6\text{As}_4\text{O}_{14}$ (Blum, Durif & Guitel, 1977), $\text{Ag}_4\text{H}_4\text{As}_4\text{O}_{14}$ (Boudjada & Averbuch-Pouchot, 1984) et $\text{Na}_3\text{H}_5\text{As}_4\text{O}_{14}$ (Driss, 1979), ils se groupent en paires liées par des tétraèdres dans la structure de $(\text{NH}_4)\text{H}_6(\text{As}_6\text{V}_4\text{O}_{14}) \cdot 4\text{H}_2\text{O}$ (Durif & Averbuch-Pouchot, 1969), ils forment un anion macromoléculaire plan dans la structure de NaHAs_2O_6 (Nguyen Huy-Dung & Jouini, 1978) et enfin s'organisent en macromolécule linéaire dans le cas présent donnant naissance à un nouveau type d'anion dans la chimie des arsénates condensés.

Références

- BLUM, D., DURIF, A. & GUILTEL, J. C. (1977). *Acta Cryst.* B33, 3222–3224.
- BOUDJADA, A. & AVERBUCH-POUCHOT, M. T. (1984). *J. Solid State Chem.* 51, 76–82.
- BRIDGMAN, P. W. (1958). *The Physics of High Pressure*. London: Bell.
- BUSING, W. R., MARTIN, K. O. & LEVY, H. A. (1979). *ORXFLS4. Crystallographic Structure-Factor Least-Squares Program*. Oak Ridge National Laboratory, Oak Ridge, Tennessee 37830, EU.
- DONNAY, G. (1970). *Am. Mineral.* 55, 1003–1015.
- DRISS, A. (1979). Thèse de Doctorat de Spécialité de Chimie Minérale. Faculté des Sciences de Tunis, Tunisie.
- DURIF, A. & AVERBUCH-POUCHOT, M. T. (1969). *Acta Cryst.* B35, 1441–1444.
- JOUINI, T. & GUÉRIN, H. (1975). *Bull. Soc. Chim. Fr.* pp. 973–975.
- NGUYEN HUY-DUNG & JOUINI, T. (1978). *Acta Cryst.* B34, 3727–3729.

Electron Density in Diammonium Hexaaquazinc(II) Sulfate – an X-ray and Neutron Study

BY E. N. MASLEN, K. J. WATSON AND S. C. RIDOUT

Department of Physics, University of Western Australia, Nedlands, Western Australia 6009, Australia

AND F. H. MOORE

Australian Institute of Nuclear Science and Engineering, Locked Mail Bag No. 1, Menai, New South Wales, Australia

(Received 24 November 1987; accepted 12 April 1988)

Abstract. An X-ray diffraction study of the electron density in $[\text{NH}_4]_2[\text{Zn}(\text{H}_2\text{O})_6](\text{SO}_4)_2$ shows the valence density around the Zn atom to be polarized sig-

nificantly by the crystal field. The differences between X-ray and neutron structural coordinates reflect the atoms' chemical environments. H atoms in strong

hydrogen bonds are shifted less than those involved in weaker bonds. Sulfate O atoms are not displaced as much as water O atoms. Charges calculated from the difference density are consistent with those for iso-morphous structures containing transition metals. Their values are small for individual atoms, but are about sixty per cent of the formal values for groups. The topography of the difference density near the Zn atom differs qualitatively from those in the corresponding copper and nickel structures. $M_r = 401.68$, monoclinic, $P2_1/a$, $a = 9.236$ (2), $b = 12.514$ (3), $c = 6.246$ (1) Å, $\beta = 106.84$ (2)°, $V = 691.0$ (2) Å³, $Z = 2$, $T = 295$ (2) K; $D_x = 1.930$ Mg m⁻³, Mo $K\alpha$, $\lambda = 0.71069$ Å, $\mu = 2.17$ mm⁻¹, $R = 0.062$ for 7297 reflections (X-ray); $\lambda = 0.9884$ Å, $\mu = 0.21$ mm⁻¹, $R = 0.062$ for 1790 reflections (neutron).

Introduction. Electron density studies on hexaaqua-magnesium, -nickel and -copper members of the $[NH_4]_2[M(H_2O)_6](SO_4)_2$ series were described by Maslen, Ridout & Watson (1988), Maslen, Ridout, Watson & Moore (1988a,b) and Maslen, Watson & Moore (1988). The topography of the difference density is not consistent with the idealized geometry for these structures. Near the metal atoms the maps do not have octahedral symmetry. Charges determined by the method of Hirshfeld (1977) are more positive for the ligating water molecules with shorter M–O bonds. The differences in charge and bond lengths are due to interaction with the ammonium group. The electron distribution associated with the 3d electrons, which is strongly affected by the exchange term in the metal-ligand interaction, is also modulated significantly by interactions beyond the first coordination sphere.

The ground states for both the Zn free atom and the Zn²⁺ ion are spherically symmetric. Their 3d¹⁰ configuration provides a reference system with which the incomplete 3d subshells of the transition metals can be compared. Zinc's chemical behaviour is often explained in terms of the resistance of the 3d¹⁰ configuration to polarization. However, in the analogous case of a filled 4f subshell, Chatterjee, Maslen & Watson (1988) observed strong polarization of the metal density. Following a refinement of the 2Zn insulin structure, Sakabe, Sasaki & Sakabe (1984) noted features characteristic of chemical bonding in the difference density near the two Zn atoms. Their angle dependence reflected the octahedral coordination of the Zn atoms, but the nearest maxima were so far from the Zn nucleus that they could not be attributed with confidence to the 3d electrons. Ohba, Shiokawa & Saito (1987) report anisotropy of the difference density near the Zn atom in ammonium tetrachlorozincate(II) chloride. Although the Zn atom in that structure is tetrahedrally coordinated, the difference density near the metal has a strong symmetric component. There are pronounced maxima in the map 0.6 Å from the Zn nucleus. The density is

depleted along the line of the Zn–Cl vectors, with minima in the $\Delta\rho$ map about 0.3 Å from the metal nucleus.

In order to gain further information on the relationship of the electron density to its bonding for zinc we studied the Tutton salt $[NH_4]_2[Zn(H_2O)_6](SO_4)_2$ by X-ray and neutron diffraction. The structure was determined originally by Montgomery & Lingafelter (1964).

Experimental. Crystals by evaporation of a water solution with equimolar concentrations of zinc and ammonium sulfates.

X-ray specimen with 12 faces and dimensions 0.24 × 0.28 × 0.36 mm parallel to [110], [001] and [110] respectively. Nicolet $P2_1$ four-circle diffractometer with graphite monochromator, Mo $K\alpha$. Cell parameters refined by least-squares refinement of 6 reflections, each measured twice, with $54 < 2\theta < 57$ °. $F(000) = 416$. Standards ± 800 , 0 ± 80 , 00 ± 4 showing 6% drift, $\sigma^2(I) = I_m + 0.00023I_m^2$. Absorption corrections by Gaussian integration with $0.58 < A < 0.65$ and minimum correction 0.92. 32925 observations reduced by averaging to 7297 unique reflections with $R_{int} = (\sum |I - \langle I \rangle|)/\sum I = 0.033$, $0 \leq h \leq 19$, $0 \leq k \leq 26$, $-12 \leq l \leq 12$, $2\theta_{max} = 100$ °. Secondary-extinction correction with $g = 0.67$ (3) (Hall & Stewart, 1987) and minimum correction factor 0.86. Atomic X-ray scattering factors and dispersion corrections from *International Tables for X-ray Crystallography* (1974). Anisotropic thermal parameters for N, O, S, Zn, isotropic for H, refined by full-matrix least squares based on F until $\Delta/\sigma < 0.01$, $R = 0.062$, $wR = 0.027$, $S = 2.044$ (2), $w = 1/\sigma^2(F)$.

Neutron data measured on the four-circle diffractometer at the AAEC Research Reactor at Lucas Heights, New South Wales. Neutron specimen with 16 faces of dimensions 2.1 × 3.1 × 5.0 mm parallel to [110], [001] and [010]. Standard reflection 404 measured after 25 ordinary reflections showed 6% drift. Cell dimensions determined from 93 reflections fully centred in the counter aperture with $13 \leq 2\theta < 62$ ° to be $a = 9.243$ (1), $b = 12.524$ (3), $c = 6.252$ (2) Å, $\beta = 106.88$ (1)°. Absorption corrections by Gaussian integration with $0.59 < A < 0.67$. 3592 measurements by $\omega-2\theta$ scan reduced to 1790 unique reflections with $-11 \leq h < 12$, $0 \leq k < 16$, $0 \leq l \leq 6$, $2\theta_{max} = 86$ °. Scattering lengths from *International Tables for X-ray Crystallography* (1974). Secondary-extinction correction with $g = 114$ (3) (Hall & Stewart, 1987) and minimum correction factor 0.51. Coordinates and anisotropic thermal parameters for all atoms refined by full-matrix least squares based on F until $\Delta/\sigma < 0.01$, $R = 0.062$, $wR = 0.043$, $S = 1.985$ (4). $w = 1/\sigma^2(F)$. The atomic coordinates are listed in Table 1, with bond lengths and angles in Table 2. The neutron and X-ray parameters are compared in Table 3, and details

Table 1. Fractional atomic coordinates and equivalent isotropic thermal parameters (\AA^2)

	$B_{\text{eq}} = (8\pi^2/3) \sum_i \sum_j U_{ij} a_i^* a_j^* \mathbf{a}_i \cdot \mathbf{a}_j$							
	X-ray ($\times 10^5$ N, O, S, Zn, $\times 10^3$ H)			Neutron ($\times 10^4$)				
	x	y	z	B_{eq}	x	y	z	B_{eq}
Zn	0	0	0	1.48	0	0	0	1.53
S(2)	40746 (2)	13701 (1)	73994 (3)	1.55	4077 (3)	1368 (2)	7399 (4)	1.61
O(3)	41216 (9)	22798 (5)	59076 (11)	2.76	4123 (2)	2278 (1)	5914 (3)	2.76
O(4)	54805 (8)	7648 (6)	78459 (14)	3.30	5479 (2)	764 (2)	7847 (3)	3.33
O(5)	27979 (7)	6700 (5)	62341 (10)	2.09	2801 (2)	674 (1)	6233 (2)	2.12
O(6)	38471 (8)	17723 (5)	95043 (10)	2.47	3848 (2)	1769 (1)	9502 (2)	2.56
O(7)	17047 (8)	10845 (6)	16559 (12)	2.18	1715 (2)	1084 (1)	1665 (2)	2.12
O(8)	-16300 (7)	11114 (5)	3452 (12)	2.19	-1636 (2)	1116 (1)	338 (3)	2.22
O(9)	83 (8)	-6799 (5)	30097 (10)	2.05	3 (2)	-682 (1)	3005 (2)	2.07
N(10)	13384 (11)	34798 (7)	35755 (15)	2.47	1337 (1)	3476 (1)	3578 (2)	2.58
H(11)	75 (2)	336 (1)	221 (3)	4.61	662 (5)	3350 (4)	2032 (6)	5.40
H(12)	206 (2)	309 (1)	384 (3)	4.20	2235 (5)	2983 (3)	3984 (8)	5.43
H(13)	85 (2)	339 (1)	449 (3)	5.10	756 (6)	3348 (5)	4668 (7)	6.91
H(14)	153 (2)	424 (1)	355 (3)	5.43	1682 (5)	4242 (3)	3645 (7)	5.02
H(15)	200 (2)	90 (1)	268 (3)	3.72	2188 (3)	914 (2)	3226 (5)	3.13
H(16)	233 (2)	121 (1)	106 (2)	3.58	2489 (3)	1237 (2)	946 (5)	3.47
H(17)	-251 (2)	99 (1)	-46 (2)	2.58	-2667 (3)	980 (2)	-563 (5)	3.24
H(18)	-148 (2)	167 (1)	20 (2)	3.23	-1421 (3)	1854 (2)	24 (5)	3.22
H(19)	-75 (2)	-63 (1)	343 (2)	3.27	-936 (4)	-601 (3)	3396 (5)	3.84
H(20)	29 (1)	-138 (1)	326 (2)	2.83	266 (3)	-1432 (2)	3255 (5)	3.10

Table 2. Bond lengths (\AA) and angles ($^\circ$)

	X-ray	Neutron	X-ray	Neutron	
Zn—O(7)	2.109 (1)	2.115 (2)	O(3)—S(2)—O(4)	109.45 (5)	109.58 (22)
Zn—O(8)	2.106 (1)	2.113 (2)	O(3)—S(2)—O(5)	108.08 (4)	107.95 (17)
Zn—O(9)	2.062 (1)	2.061 (2)	O(3)—S(2)—O(6)	109.62 (5)	109.56 (19)
S(2)—O(3)	1.480 (1)	1.477 (3)	O(4)—S(2)—O(5)	108.96 (4)	109.11 (20)
S(2)—O(4)	1.459 (1)	1.456 (3)	O(4)—S(2)—O(6)	110.77 (5)	111.75 (18)
S(2)—O(5)	1.480 (1)	1.476 (3)	O(5)—S(2)—O(6)	109.92 (4)	109.85 (22)
S(2)—O(6)	1.478 (1)	1.477 (3)	H(11)—N(10)—H(12)	110.0 (16)	112.7 (4)
N(10)—H(11)	0.882 (16)	0.998 (4)	H(11)—N(10)—H(13)	109.3 (16)	109.1 (4)
N(10)—H(12)	0.799 (17)	1.005 (4)	H(11)—N(10)—H(14)	102.7 (14)	107.0 (4)
N(10)—H(13)	0.831 (20)	0.995 (6)	H(12)—N(10)—H(13)	110.6 (16)	107.3 (4)
N(10)—H(14)	0.968 (17)	1.008 (4)	H(12)—N(10)—H(14)	117.1 (16)	110.2 (4)
O(7)—H(15)	0.659 (15)	0.970 (3)	H(13)—N(10)—H(14)	106.7 (16)	110.6 (4)
O(7)—H(16)	0.786 (18)	0.967 (4)	Zn—O(7)—H(15)	106.8 (12)	114.2 (2)
O(8)—H(17)	0.833 (12)	0.971 (3)	Zn—O(7)—H(16)	116.0 (10)	116.6 (2)
O(8)—H(18)	0.729 (13)	0.977 (3)	H(15)—O(7)—O(16)	112.2 (18)	109.4 (3)
O(9)—H(19)	0.817 (17)	0.972 (4)	Zn—O(8)—H(17)	114.4 (9)	115.9 (2)
O(9)—H(20)	0.916 (12)	0.971 (3)	Zn—O(8)—H(18)	117.2 (12)	114.3 (2)
O(7)—Zn—O(8)	88.80 (4)	89.00 (6)	H(17)—O(8)—H(18)	107.0 (13)	105.8 (3)
O(7)—Zn—O(9)	90.77 (3)	90.82 (7)	Zn—O(9)—H(19)	118.9 (9)	114.8 (2)
O(8)—Zn—O(9)	89.60 (3)	89.71 (7)	Zn—O(9)—H(20)	118.5 (8)	118.8 (2)
			H(19)—O(9)—H(20)	104.4 (13)	105.0 (3)

relevant to the hydrogen-bond system are given in Table 4.*

Discussion.

Structural properties

The packing and hydrogen-bond system for the hexaaqua members of the Tutton-salt structures have been described by Montgomery & Lingafelter (1966). For the series generally, the M—O(9) bond is the shortest metal-ligand bond and, except for transition-metal structures affected by Jahn-Teller distortion, the M—O(7) and M—O(8) bond lengths are almost equal, as is evident in Table 2. The S—O(4) length is significantly shorter than the lengths of the corresponding bonds to O(3), O(5) and O(6) which are the

acceptors for strong N—H···O hydrogen bonds as seen from Table 4.

Among the H atoms, the X—N shifts are notably smaller for the H(11), H(14), H(17) and H(20) atoms which are involved in strong hydrogen bonds. A more symmetrical distribution of the electron density is expected for these atoms because the antisymmetric component of the potential for the covalently bonded H atom is partly compensated by the contribution from the strong hydrogen bond. The mean X—N shift for the water O atoms is larger than that for the sulfate O atoms, continuing the trend observed at a higher level of significance in the magnesium structure (Maslen, Ridout, Watson & Moore, 1988a). In the case of oxygen this shift reflects the lone-pair development. That for the sulfate O atoms is reduced by lone-pair involvement in strong O—H···O hydrogen bonds.

Difference density

A difference density was evaluated. Atomic charges, determined from the difference density by the method of

* Lists of structure factors and anisotropic thermal parameters have been deposited with the British Library Document Supply Centre as Supplementary Publication No. SUP 44961 (27 pp.). Copies may be obtained through The Executive Secretary, International Union of Crystallography, 5 Abbey Square, Chester CH1 2HU, England.

Table 3. Comparison of X-ray (*X*) and neutron (*N*) structures

<i>X</i>	<i>N</i>	Distance (Å)	<i>X</i>	<i>N</i>	<i>N</i>	Angle (°)
S(2)–S(2)		0.003 (3)	O(7)–O(7)–Zn			48 (10)
O(3)–O(3)		0.004 (2)	O(7)–O(7)– <i>B7*</i>			170 (11)
O(4)–O(4)		0.002 (2)	O(8)–O(8)–Zn			36 (14)
O(5)–O(5)		0.006 (2)	O(8)–O(8)– <i>B8*</i>			171 (14)
O(6)–O(6)		0.004 (2)	O(9)–O(9)–Zn			98 (19)
O(7)–O(7)		0.009 (2)	O(9)–O(9)– <i>B9*</i>			124 (19)
O(8)–O(8)		0.008 (2)	O(3)–O(3)–S(2)			155 (23)
O(9)–O(9)		0.005 (2)	O(4)–O(4)–S(2)			95 (50)
N(10)–N(10)		0.005 (1)	O(5)–O(5)–S(2)			143 (14)
H(11)–H(11)		0.117 (16)	O(6)–O(6)–S(2)			135 (24)
H(12)–H(12)		0.213 (16)	H(11)–H(11)–N(10)			6 (8)
H(13)–H(13)		0.168 (20)	H(12)–H(12)–N(10)			10 (5)
H(14)–H(14)		0.138 (18)	H(13)–H(13)–N(10)			7 (5)
H(15)–H(15)		0.336 (15)	H(14)–H(14)–N(10)			71 (7)
H(16)–H(16)		0.186 (18)	H(15)–H(15)–O(7)			16 (2)
H(17)–H(17)		0.145 (13)	H(16)–H(16)–O(7)			5 (4)
H(18)–H(18)		0.263 (14)	H(17)–H(17)–O(8)			11 (5)
H(19)–H(19)		0.173 (16)	H(18)–H(18)–O(8)			14 (3)
H(20)–H(20)		0.066 (13)	H(19)–H(19)–O(9)			22 (5)
			H(20)–H(20)–O(9)			31 (11)

* *B7*, *B8* and *B9* are the internal bisectors of the H–O–H angles centred on O(7), O(8) and O(9) respectively.

Table 4. Hydrogen-bond distances (Å) and angles (°) from the neutron structure

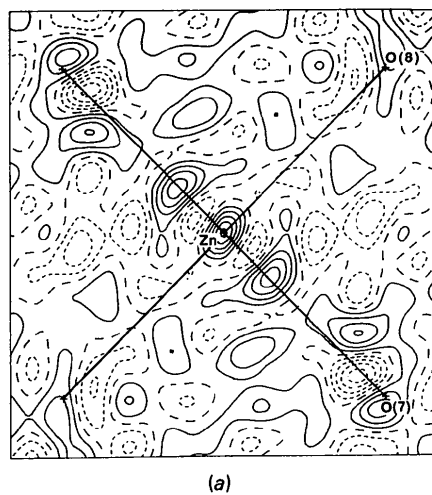
Bond <i>A</i> –H… <i>B</i>	Distance <i>A</i> … <i>B</i>	Equivalent position*	Angle <i>A</i> –H… <i>B</i>
O(7)–H(15)…O(5)	2.785 (2)	<i>x</i> , <i>y</i> , <i>z</i>	170.9 (3)
O(7)–H(16)…O(6)	2.826 (2)	<i>x</i> , <i>y</i> , <i>z</i> –1	170.2 (3)
O(8)–H(17)…O(4)	2.704 (2)	<i>x</i> –1, <i>y</i> , <i>z</i> –1	178.8 (3)
O(8)–H(18)…O(6)	2.759 (3)	<i>x</i> – $\frac{1}{2}$, $\frac{1}{2}$ – <i>y</i> , <i>z</i> –1	175.7 (3)
O(9)–H(19)…O(5)	2.766 (2)	– <i>x</i> , – <i>y</i> , 1– <i>z</i>	168.8 (3)
O(9)–H(20)…O(3)	2.704 (2)	$\frac{1}{2}$ – <i>x</i> , $\frac{1}{2}$ – <i>y</i> , 1– <i>z</i>	171.9 (3)
N(10)–H(11)…O(6)	2.910 (2)	<i>x</i> – $\frac{1}{2}$, $\frac{1}{2}$ – <i>y</i> , <i>z</i> –1	161.1 (4)
N(10)–H(12)…O(3)	2.971 (2)	<i>x</i> , <i>y</i> , <i>z</i>	158.2 (4)
N(10)–H(13)…O(3)	2.988 (2)	<i>x</i> – $\frac{1}{2}$, $\frac{1}{2}$ – <i>y</i> , <i>z</i>	157.9 (4)
N(10)–H(13)…O(4)	3.142 (3)	<i>x</i> – $\frac{1}{2}$, $\frac{1}{2}$ – <i>y</i> , <i>z</i>	135.6 (4)
N(10)–H(14)…O(5)	2.856 (2)	$\frac{1}{2}$ – <i>x</i> , $\frac{1}{2}$ + <i>y</i> , 1– <i>z</i>	176.5 (4)

* Symmetry operation for the receptor atom *B*.

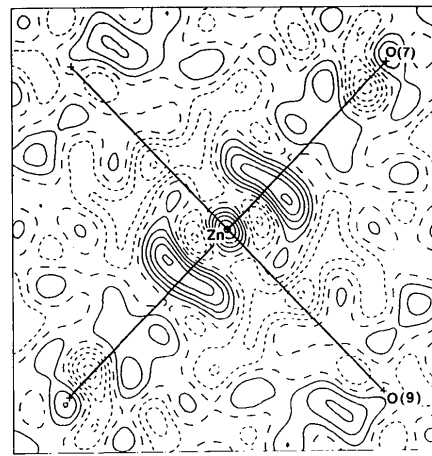
Table 5. Atomic charges, as defined by Hirshfeld (1977)

Atom	Group	Charge	Atom	Group	Charge
Zn		0.43 (6)	N(10)		0.17 (3)
O(7)		–0.02 (2)	H(11)		0.16 (2)
H(15)		–0.02 (2)	H(12)		–0.10 (2)
H(16)		0.13 (2)	H(13)		0.05 (2)
	H ₂ O	0.09	H(14)	NH ₄	0.11 (2)
O(8)		–0.06 (2)	S(2)		0.16 (3)
H(17)		–0.07 (2)	O(3)		–0.36 (2)
H(18)		–0.00 (2)	O(4)		–0.25 (2)
	H ₂ O	–0.13	O(5)		–0.31 (2)
O(9)		0.16 (2)	O(6)		–0.25 (2)
H(19)		0.16 (2)	SO ₄		–1.01
H(20)		0.14 (2)		Zn(H ₂ O) ₆	1.26
	H ₂ O	0.46			

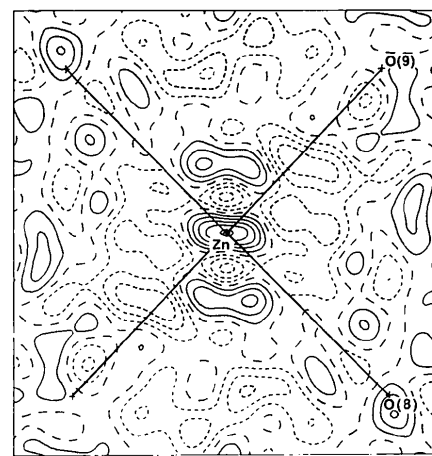
Hirshfeld (1977), are listed in Table 5. In this method the difference density at \mathbf{r} is assigned to the *i*th atom with a weight $w_i = \rho_i^{\text{at}}(\mathbf{r})/\rho^{\text{pro}}(\mathbf{r})$, where ρ_i^{at} is the free-atom density for the *i*th atom and the sum for all atoms is the promolecule density ρ^{pro} . The charges of 1.26, 0.39 and –1.01 electrons for the hexaaquametal moiety, the ammonium group and the sulfate group resemble the corresponding values of 0.91, 0.61 and –1.10 electrons for the magnesium structure. The water molecule containing O(9) carries the largest



(a)



(b)



(c)

Fig. 1. Residual density for (a) the Zn–O(7)–O(8) plane, (b) the Zn–O(7)–O(9) plane, (c) the Zn–O(8)–O(9) plane. Contour interval 0.15 e Å^{–3}. Zero contour broken. Negative contours dotted. Map area 4.0 × 4.0 Å.

positive charge, as was also found in the magnesium and nickel structures.

Although the atomic and group charges are similar for the structures, the topography of the difference density differs markedly from those for the transition metals. The topographies of the sections of the difference density near the Zn nucleus in the three maps shown in Fig. 1 are minor variations on the one theme. An elongated peak or ridge of density straddles the metal nucleus. A localized minimum 0.3 Å from the nucleus extends in a direction normal to the ridge, with positive density in approximately the same direction, reaching a maximum 0.6 Å from the nucleus. However, the relationships of these features to the Zn–O bonds is quite different, with the approximate symmetry axes for the feature aligned along the bonds in (a) and bisecting the O–Zn–O angle in (c). The orientation in (b) is intermediate between these two orientations, but closer to that in (a). In Figs. 1(b) and 1(c) containing O(9), the central ridge points towards a broad depleted region intersecting with, and reaching a minimum on, the Zn–O(9) vector. The density along M–O(9) is also depleted in the magnesium, nickel and copper complexes. However, this region is more extensive in the zinc structure.

For the transition-metal complexes there are minima, 0.3 Å from the metal nucleus and aligned closely with M–O(7) and M–O(8), which are attributed to the reduction of density in the e_g orbitals. Although there are minima at about 0.3 Å from the Zn nucleus, these do not minimize along the M–O bonds. There is strong concentration of density 0.6 Å from the metal nucleus, especially along the Zn–O(7) bond. The appearance of

the map suggests that it is constructed from components with a radial structure such that the sign of the difference density changes between 0.3 and 0.6 Å from the metal.

The authors acknowledge the assistance of A. H. White with the X-ray measurements. Computer programs for the data reduction and structure analysis were from the *XTAL* system of Hall & Stewart (1987).

References

- CHATTERJEE, A., MASLEN, E. N. & WATSON, K. J. (1988). *Acta Cryst. B44*, 381–386, 386–395.
 HALL, S. R. & STEWART, J. M. (1987). *XTAL2.2 User's Manual*. Univs. of Western Australia, Australia, and Maryland, USA.
 HIRSHFELD, F. L. (1977). *Theor. Chim. Acta*, **44**, 129–138.
International Tables for X-ray Crystallography (1974). Vol. IV. Birmingham: Kynoch Press. (Present distributor Kluwer Academic Publishers, Dordrecht.)
 MASLEN, E. N., RIDOUT, S. C. & WATSON, K. J. (1988). *Acta Cryst. B44*, 96–101.
 MASLEN, E. N., RIDOUT, S. C., WATSON, K. J. & MOORE, F. H. (1988a). *Acta Cryst. C44*, 409–412.
 MASLEN, E. N., RIDOUT, S. C., WATSON, K. J. & MOORE, F. H. (1988b). *Acta Cryst. C44*, 412–415.
 MASLEN, E. N., WATSON, K. J. & MOORE, F. H. (1988). *Acta Cryst. B44*, 102–107.
 MONTGOMERY, H. & LINGAFELTER, E. C. (1964). *Acta Cryst. 17*, 1295–1299.
 MONTGOMERY, H. & LINGAFELTER, E. C. (1966). *Acta Cryst. 20*, 659–662.
 OHBA, S., SHIOKAWA, K. & SAITO, Y. (1987). *Acta Cryst. C43*, 189–191.
 SAKABE, M., SASAKI, K. & SAKABE, K. (1984). *Methods and Applications in Crystallographic Computing*, edited by S. R. HALL & T. ASHIDA, pp. 273–285. Oxford: Clarendon Press.

Acta Cryst. (1988). **C44**, 1514–1516

Structure du Tétraméthyl-3,3',4,4' Tétrathia-2,2',5,5' Fulvalénium Tétracyanonickelate(II): $(\text{TMTTF})_2[\text{Ni}(\text{CN})_4]$

PAR MUSTAPHA BENCHARIF ET LAHCÈNE OUAHAB*

Laboratoire des Matériaux Moléculaires et de Cristallochimie, Institut de Chimie, Université de Constantine,
Algérie

(Reçu le 6 juillet 1987, accepté le 5 avril 1988)

Abstract. $[\text{C}_{10}\text{H}_{12}\text{S}_4]_2[\text{Ni}(\text{CN})_4]$, $M_r = 683.71$, triclinic, $P\bar{1}$, $a = 8.186(4)$, $b = 8.574(4)$, $c = 10.361(6)$ Å, $\alpha = 92.54(6)$, $\beta = 97.47(6)$, $\gamma = 98.14(7)^\circ$, $V = 712.3$ Å 3 , $Z = 1$, $D_x = 1.594$ g cm $^{-3}$, $\lambda(\text{Mo } K\alpha) = 0.71073$ Å, $\mu = 12.70$ cm $^{-1}$, $F(000) =$

352, $T = 293$ K, $R = 0.038$ for 1705 observed reflections. The TMTTF molecules are dimerized and form with the $\text{Ni}(\text{CN})_4$ a distorted cubic coordination typical of the CsCl structure type. The $\text{Ni}(\text{CN})_4$ anions form a dihedral angle of 102.1° with the TMTTF. The 2:1 stoichiometry suggests fully oxidized organic molecules in agreement with the insulating character of this material.

* Auteur auquel correspondance devra être adressée.